Journal of the European Ceramic Society, Volume 29, Issue 13, October 2009, Pages 2799–2805

Influence of annealing on the photochemical deposition of silver onto PZT thin films under UV irradiation

Divya Tiwari, Steve Dunn

Nanotechnology Centre, Bldg. 30, Cranfield University, Beds, MK43 0AL, UK

Abstract

Silver nanoparticle deposition from an aqueous solution of 0.01 M silver nitrate solution onto the c^+ domain of PZT (30/70) thin films has been investigated for samples annealed at a variety of temperatures from 530 to 690 °C. The impact of annealing was to increase the deposition of photoreduced silver on the surface. When the PZT samples were annealed in air at temperatures ranging from 530 to 690 °C the silver deposition increased by more than 200%. The increase in the deposition of the silver is attributed to increase in the defect concentration due to the volatilisation of components from the PZT, most importantly PbO. Variations in the Pb concentration of the sample are measured using EDX and show a marked change, reduction in Pb, with annealing temperature.

1. Introduction

Over the past few years there has been an increase in the interest in the use of ferroelectric materials as photocatalysts, or their use in photochemistry. The historical perspective of the semiconducting nature of ferroelectric materials is the natural pre-cursor to investigating the photochemistry. What is most interesting is the use of patterns on ferroelectric surfaces that can be used for spatially selected chemical reactions. Initially Giocondi and Rohrer[1] demonstrated that it was possible to spatially separate the reduction and oxidation processes on the surface of a ferroelectric material using barium titanate. This was quickly followed by the work of Kalinin et al.[2] who developed an interesting approach for the growth of nanostructures of metals which they called 'ferroelectric nanolithography'. The technique highlighted the possibility of growing metallic nanostructures on predefined locations of a ferroelectric surface. The exact location of surface reaction was defined by the availability of photoexcited carriers at the surface of the ferroelectric. Either electrons for reduction or holes for oxidation of solvated species. The selective deposition process is attributed to the interaction between the space charge region (SPR) developed in the ferroelectric resulting from the internal dipole formed by the displacement of ions in the crystal lattice. The SPR induces photoexcited carriers to separate near the surface; electrons to migrate to the surface on a c^+ domain while holes migrate to the surface on a $c-$ domain.

When a photosensitive material, such as a ferroelectric, is exposed to super band gap irradiation photoexcited charge carriers ($e-$–h^+) pairs are generated.[3] These charge carriers are established in the ferroelectric material and driven apart by the internal electric field in the SPR. As described earlier in positively polarized domains electrons are forced to migrate towards the surface[4] and in negatively

polarized domains electrons move away from the surface and towards the bulk. In the vicinity of surfaces and interfaces of ferroelectric materials a polarisation bound charge σ exists which is:

$$\sigma = P \cdot n \quad (1)$$

where σ is surface or polarisation charge, ***P*** is polarisation vector and ***n*** is unit vector normal to the surface. This induced surface charge may be compensated by two possible mechanisms – internal and external screening. External screening involves surface adsorption of oppositely charged molecules or ions on the surface of the ferroelectric. Internal screening involves compensation of surface polarisation charge free charge carriers that result from defects in the material structure. In the case of internal screening mechanisms this results in 'band bending' at the surface of the ferroelectric material.[5] In turn there is a formation of depletion and accumulation layers that are dependent on the nature of ferroelectric domain. Crucially these are, largely, independent of the position of the Fermi level or REDOX couple that is in contact with the ferroelectric and are inherent in any poled ferroelectric system.

When the ferroelectric is covered in a silver salt (AgNO3) solution and exposed to super band gap irradiation metal cations can react with the photoexcited electrons available on the positive domains and become reduced to metal. There are several very interesting aspects to the growth of the silver on the positively poled domain. The most important is that the Ag^+ ions will not be intimately attached to the c^+ surface. In fact the negatively charged counter ions will form a Stern or double layer at the surface of the c^+ domain due to Helmholtz theory. Therefore, in order for the photoexcited electron in the conduction band of the PZT to interact with the metal cation it must tunnel from the PZT surface through the screening layer to reach the cation.

The growth of photochemical metallic nanostructures on ferroelectric materials has been shown to be dependent on a number of surface phenomena. These include features such as grain boundaries,[6] ferroelectric domains[2,7] and domain boundaries.[8] In each of these cases there is an interaction between the SPR that is forming due to a boundary effect and the photoexcited carriers. This means it is now accepted that ferroelectric materials can be considered and treated as wide band gap semiconductors[9] exhibiting domain specific photochemical behavior.

There are further complications when considering the photochemical reactivity of ferroelectric surfaces. These are that the surface reactivity is not only dependent on polarisation of domain[1] but also the crystallographic orientation of the sample.[10] The underpinning materials properties can also impact on the surface photochemistry as it has been shown that the density of defects in the sample can have a major impact on the photochemical reactivity, as demonstrated by Hanson et al.[8] In this case silver was preferentially depositing by the photoreduc-tion reaction on the domain boundaries. This selective deposition on the LiNbO3 surface was attributed to the low concentration of defect states near the surface (10^{12} cm^{-2}).[7,11]

As we have discussed earlier, defects contribute to internal screening. Therefore a low concentration of defects leads to weak internal screening. This weak internal screening means that the material becomes dependent on external screening for compensation of surface charges. The result of this is a tightly bound and highly structured Stern layer that presents a larger barrier to tunneling than in the case

of a material that is predominantly internally compensated. In the case of PZT where there is significant internal screening then there will only be loose counter ion screening. This will significantly increase the probability of a carrier successfully tunneling. For LiNbO3 the tight screened layer is such that only large discontinuities of local electric field, *i.e.* a domain boundary are sufficiently strong to disrupt the local Stern layer and allow for tunneling of carriers that can perform REDOX chemistry.[12]

In PZT films, when a domain patterned surface is dipped in metal salt solution and exposed to super band gap irradiation silver nanoparticle deposition occurs over the entire c^+ domain. The difference in photochemical reactivity of PZT compared to LiNbO3 is attributed to high density of defects present on the PZT surface. During the annealing of PZT films defects are introduced and therefore the defect density of PZT films is higher (10^{14} cm^2)[9] than for LiNbO3. Higher defect density leads to predominantly internal screening resulting in strong band bending and a thin SCR. Upon exposure to super band gap illumination electron–hole pairs are generated across a deep region. The electric field associated with strong band bending results in efficient separation of electrons and holes and a large number of electrons can reach the surface of c^+ domains leading to silver nanoparticle deposition on c^+ domains.

In summary, the density of defects in a ferroelectric material has an impact on the photochemical reactivity at its surface. This is due to the interaction with the band structure that arises from the development of new defect states and the associated mobile carriers. Unfortunately, information on defect chemistry for thin film perovskites has not been fully investigated due to difficulties in developing suitable measurement tools at the high defect densities associated with many perovskite systems. Here, we have investigated the impact of annealing and increasing the defect concentration in PZT thin films on the photochemistry of PZT. When the PZT samples were annealed in air at temperatures ranging from 530 to 690°C the silver nanoparticle deposition increased by more than 200%. The increase in the deposition of the silver is attributed to increase in the defect concentration (mainly oxygen vacancies) at the surface of the PZT and the change in the band structure at the surface.

2. Experimental procedure

A PZT film with the Zr/Ti ratio of 30/70 was made using a sol–gel process. The sol was prepared according to previously published work[13] and spin coated onto a prepared substrate of Pt (100 nm)/Ti (5 nm)/SiO2 (450 nm)/Si. The PZT film was 70 nm thick and was 2 cm^2 in area. Film orientation was determined using X-ray diffraction (XRD) 0−20 measurement on a Siemens D5005 diffractometer using CuKa radiation. The sample exhibited good ferroelectric properties as determined by hysteresis loop measurements using an RT66A. The PZT sample was then cut into four pieces of equal size. One of the four pieces was kept as it was and the rest were annealed separately in a furnace under air at temperatures of 590, 630 and 690°C for 30 min. The samples were then poled using a modified DI 3000 Atomic Force Microscope (AFM) system in PFM[14] mode using a conductive cantilever (a Veeco contact mode cantilever made of Antimony doped Si, resonant frequency 130–250 kHz) and supplying 12 V between the cantilever and base electrode. The base electrode of the sample was obtained by scratching a part of the sample and connecting a wire using silver loaded glue. For positive

domains the tip was held negative against ground and for negative domains the tip was held positive. The pattern produced was a series of squares of reduced dimensions set inside each other of opposite domain orientation.

A fresh solution of 0.01 M AgNO3 was prepared by mixing AgNO3 (Aldrich 99.99%) with deionized water. A drop of this solution was put over the poled pattern in the sample. The sample was then irradiated with a UV lamp (Honle 400W Hg lamp) for 20 min. After irradiation the samples were rinsed in deionized water and blown dry with N2. The samples were imaged using a Philips XL30 SFEG scanning electron microscope (SEM) in high resolution mode. The percentage deposition of silver nanoparticles on the surface was determined using energy dispersive X-ray analysis (EDAX) technique on the Philips XL30 SFEG.

3. Results and discussion

As determined by XRD the PZT 30/70 films exhibited a [1 1 1] orientation, as shown in Fig. 1. The XRD also shows an absence of any intermediate pyrochlore phase in the samples as was supported by the P/E loop generated by the sample. The XRD patterns for all samples after annealing are compared, shown in Fig. 1, and no change was found in the XRD pattern with respect to annealing temperature.

Before poling the PZT was investigated using Piezo force microscopy (PFM) and shown to consist of discrete grains with a random orientation across the surface. PFM was then used to write positive (c^{+}) and negative (c−) domain patterns in the form of squares as shown in Fig. 2 (left). Brighter squares in the picture are positive domains and the dark squares are negative domains, the surrounding region is an unpoled area showing the random orientation of the as produced film. This has a periodicity in the order of the crystallite size of 70–100 nm. After poling an area on the PZT surface in the form of squares, a drop of freshly made silver nitrate salt solution which was filtered using a 0.2 pm filter was placed over the poled area. A typical SEM image of photodeposited silver is shown in Fig. 2 (right).

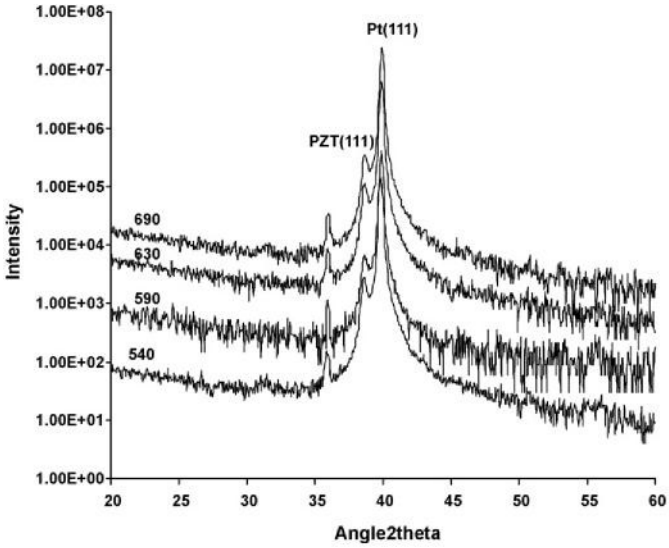


Fig. 1. A comparison of XRD patterns for samples annealed at temperatures 540, 590, 630 and 690 °C. ***X***-axis is the angle in 2θ (◦) and ***Y***-axis is the intensity in counts.

The band gap of PZT material has been reported to range from 3.2 to 3.7 eV.[15] According to Kalinin et al.[16] energy above 4.5 eV is required for the photoreduction of Ag on the surface of PZT. The increase in irradiation energy over and above the band gap energy is described as a feature of the interaction between the flux of photons and PZT as well as chemical losses. The emission spectrum for the UV lamp used in these experiments showed that there is a significant flux of photons that are above the band gap energy and the energy required for the photoreduction of Ag. On all the PZT samples upon irradiation deposition of silver occurred only on c^+ domains and no deposition was observed on c− domains.

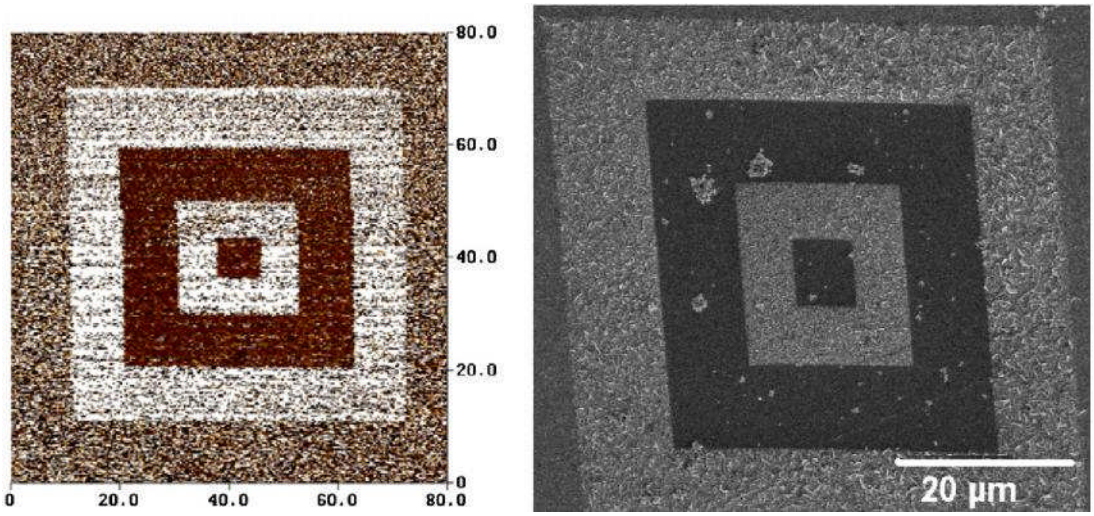


Fig. 2. A typical PFM image (left) of a typical poled pattern; brighter squares in the picture are positive domains and the dark squares are negative domains; surrounding region is an unpoled area. The scale bar shows the length in micrometer. A typical SEM image (right); silver is deposited on c^+ domains and no deposition occurred on c− domains.

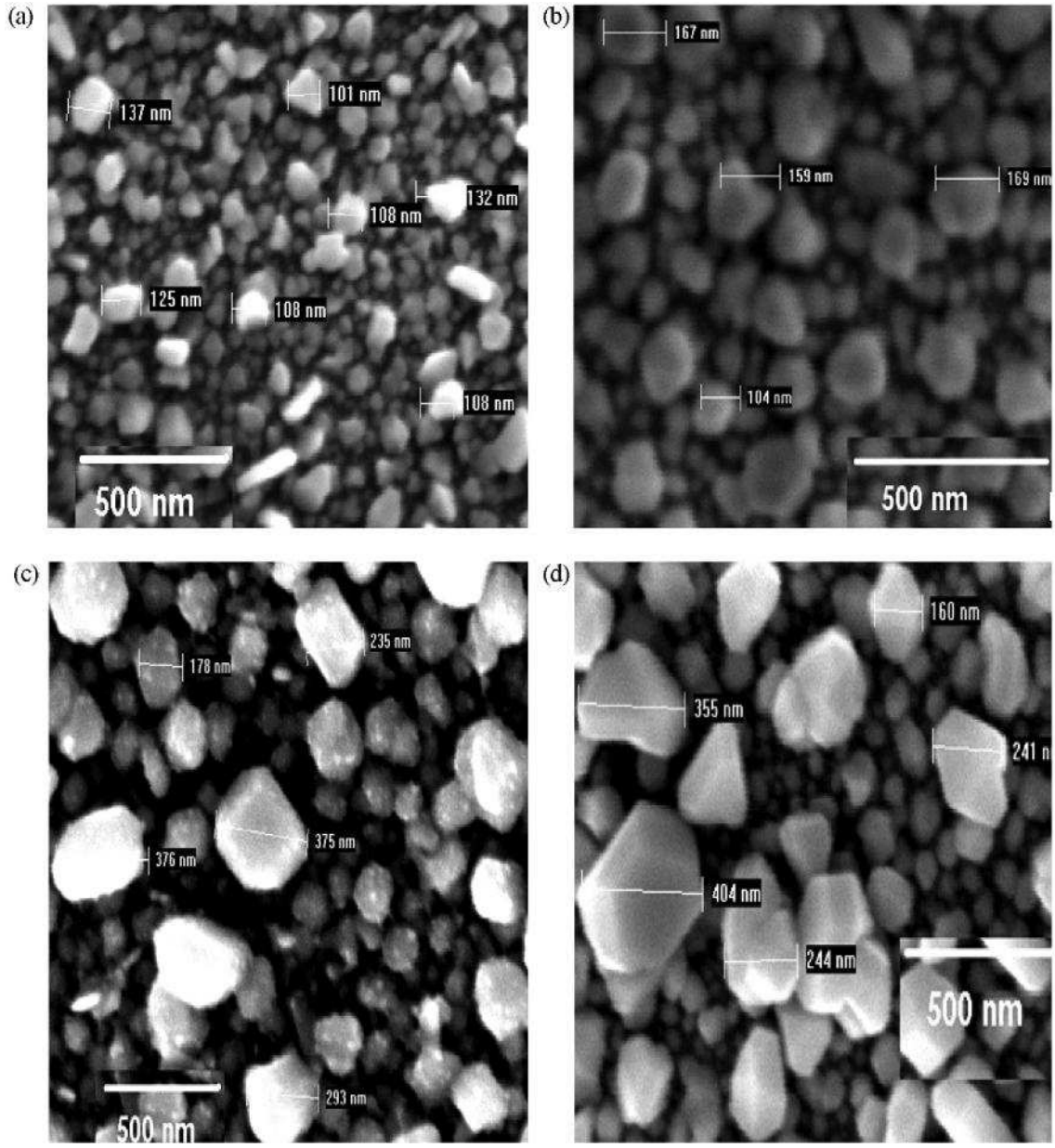


Fig. 3. SEM images after silver deposition of samples annealed at 540˚C (a), 590˚C (b), 630˚C (c) and 690˚C (d). Note the increase in the size Ag clusters on c_+ domains.

The presence of Ag was confirmed using EDX. The EDX software was calibrated using a standard Co sample. The percentage deposition of Ag was calculated in defined areas on all samples after annealing. Examination of the samples under SFEG clearly showed that the deposition of Ag nanoparticles increased as the temperature of annealing increased from 540 to 690 ˚C. These experiments were repeated for a variety of PZT samples and the range of percentage of silver, as determined using EDX, deposited on the samples was plotted, as shown in Fig. 4. A clear trend can be seen that with the increase in annealing temperatures the amount of Ag increases. The particle size of silver clusters deposited also increases with the increase in annealing temperatures as shown in Fig. 3. As there have been no changes to the PZT other than the anneal temperature this increase in the amount of Ag deposited must be due to changes associated with the high temperature anneal. It is known that PbO can volatize from the surface of PZT and high

temperature processing is either performed under a high vapour pressure of PbO or excess PbO is added to the starting material to accommodate loss during processing. We believe that the observed increase in Ag deposition on the PZT surface is due to an increase in the lattice defect concentration, due to volatisation of components (PbO) in the PZT during the annealing. It is also possible that thermal cycling could have altered the band gap due to a loss of PbO making the system non-stoichiometric with respect to lead. However, this affect was discounted as band gap measurements for the annealed samples using spectroscopic elipsometry showed no change in the band gap for the materials in the as produced or annealed states (Fig. 4).

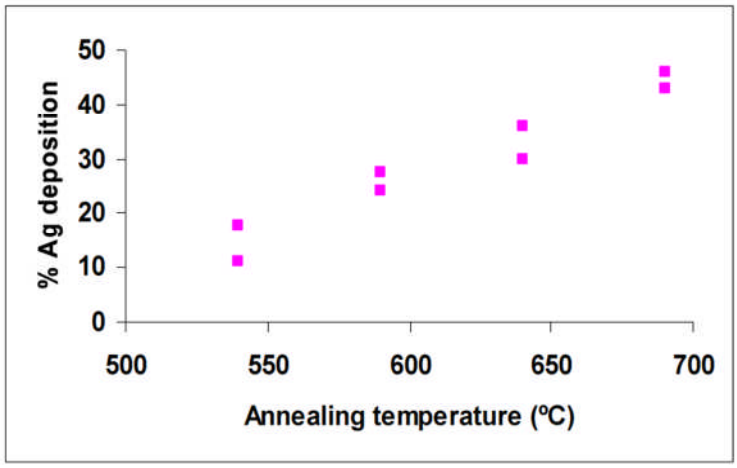


Fig. 4. Percentage deposition of silver on PZT surface plotted with respect to annealing temperatures. The two points in the plot show the range in which the percentage deposition was observed at a particular temperature.

Therefore, we are forced to look into other factors that could be affecting the band structure and hence the deposition of photochemical silver in nanostructures on the surface. According to defect chemistry a non-doped PZT film is a p-type semiconductor[9] since the naturally occurring impurities found in the material are acceptor impurities, such as Al^{3+}, Na^{+} and Fe^{3+}. PZT contains two volatile components Pb and O. During crystallisation annealing at high temperatures PbO volatilizes from the film leading to the creation of lead and oxygen vacancies. These vacancies are mainly at the surface due to the low mobility of lead through the lattice. When annealing under an oxidative atmosphere ($P_{O2\ atmos} > P_{O2\ PZT}$) some oxygen is absorbed into lattice as shown in Eq. (2)[17]:

$$\tfrac{1}{2}\, O_2 + Vo^{\cdot\cdot} = Oo + 2h^{\cdot} \qquad (2)$$

Two holes are produced in this process which are trapped on the doubly negatively charged lead vacant sites, caused by evaporation of lead, leading to the formation of singly negatively charged complexes as shown in Eq. (3).[18] $Vo^{\cdot\cdot}$ and $(V_{Pb}^{2+})''$ can also combine to form electrostatically bound complexes as shown in Eq. (4):

$$(V_{Pb}^{2+})'' + h^{\cdot} = [(V_{Pb}^{2+})''h^{\cdot}]' \qquad (3)$$

$$Vo^{\cdot\cdot} + (V_{Pb}^{2+})'' = (Vo^{\cdot\cdot}V_{Pb}'') \qquad (4)$$

Therefore, we have (acceptor–hole), (lead vacancy–hole), (lead vacancy–oxygen vacancy) complexes in the system and some mobile un-associated oxygen vacancies. Oxygen vacancies are positively charged and they produce shallow levels in the band gap which act as donors.[19] The oxygen vacancies introduce shallow level traps close to the conduction band as shown in Fig. 5.

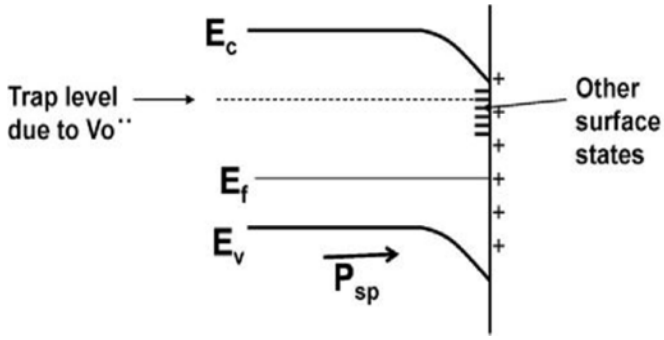


Fig. 5. Trap levels introduced due to oxygen vacancies and surface states on a c+ domain. E_v is the top of the valence band associated with oxygen 2p orbitals and E_c is bottom of conduction band associated with titanium 3d orbitals. P_{sp} arrow represents the direction of spontaneous polarisation.

Ayguavives et al.[20] have used ^{18}O depth profiling technique to study the oxygen diffusion in PZT thin films annealed at various temperatures. They have found that a strong depletion of oxygen occurs after annealing and this loss increases with the increase in annealing temperature. Although some oxygen is gained during the annealing process (according to Eq. (2)) the overall amount of O content in films decreases as the temperature of annealing is increased. Therefore, we can say that as our PZT samples are annealed at increasingly higher temperatures more PbO evaporates from the surface leading to an increase in Pb and O vacancies. This fact is also supported by the increase in electrical conductivity of PZT when the temperature was increased from 500 to 700°C under the same atmosphere[20] which is a result of the increase in low energy defect states. Similarly steady-state leakage current density of PZT thin film increased by a factor of 10^3 when annealed at high temperatures[20]; the presence of oxygen vacancies is directly attributed to the high film conductance. EDX analysis of the PZT samples was undertaken which reveals the percentage composition of different elements in the PZT samples. We are mainly interested in the relative percentage of Pb present in all the samples, plotted in Fig. 6, which confirms the loss of Pb with respect to annealing temperatures. The total loss of Pb from the entire film is about 7%. PbO evaporates from the surface, due to the low mobility of Pb in the lattice; therefore most of Pb loss occurs on the surface of PZT film leaving the large numbers of unit cells on the surface defected.

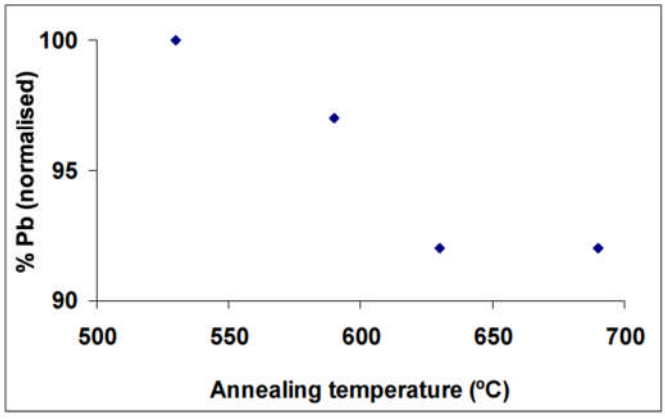


Fig. 6. Percentage of Pb (normalised) with respect to annealing temperatures.

The increase in defect concentration with respect to annealing temperature creates shallow localised energy levels in the forbidden gap as shown in Fig. 5. These shallow defect states are capable of trapping photogenerated electrons during UV illumination. This will have the effect of decreasing the energy required for activation of the electron to energy where it can perform chemistry and also increasing the lifetime of available electrons in the system. Under super band gap illumination the material is in a highly non-equilibrium situation – there are large numbers of electron–hole pairs being formed due to the interaction with the incident radiation. There are a number of ways that the photogenerated carriers in this non-equilibrium situation can recombine. One of which is through a REDOX couple which occurs on the surface of the ferroelectric material. On a c+ domain these electrons are easily available for the photoreduction of Ag^{+} to Ag^{0}. Therefore with the increase in shallow trap levels, more electrons are trapped that are able to participate in the silver photoreduction reaction. Therefore, we get an increase in silver nanocluster deposition on the surface of c^{+} domain. The higher flux of available electrons for photoreactions leads to the generation of particles of larger size. That is why we see an increase in size of silver clusters on the c^{+} domain. On a c− domain the negative polarisation charge at the surface and the direction of internal field does not allow the trapped electrons to reach the surface. In this case they are not able to participate in photochemical reactions. For this reason we do not see any photoreduced silver on the surface of negative domains.

The band structure at the surface of PZT changes due to variations in annealing at higher temperatures. As we have discussed earlier oxygen vacancies, lead vacancies and free charge carriers contribute to internal screening which compensates the polarisation bound charge at the surface. With the increase in defects the internal screening of the surface charge improves leading to a reduction in the width of space charge region[21] and eventually a change in band structure at the surface. The following expression is derived from Poisson's equation and gives the relationship between the depletion width and the dopant density for an n-type semiconductor immersed in an electrolyte solution[22].

$$W = \sqrt{\frac{2\varepsilon_s\left[E\left(A/A^{-}\right) - E_{cb} - kT\ln\frac{N_c}{N_d}\right]}{q^2 N_d}} \tag{5}$$

Where W is the depletion layer width, ε_s is the static dielectric constant of the material, $E(A/A-)$ is the electrochemical potential of the electrolyte phase, E_{cb} energy of conduction band, N_c is the effective density of states in the conduction band, N_d is the dopant density, q is the electronic charge. Therefore, as the defect density (mainly due to oxygen vacancies) increases the width of the SCR reduces. However, the SCR is still sufficiently large to enable effective separation of photogenerated holes and electrons due to the domains in the ferroelectric. This is shown by SEM images of photoreduced silver on samples annealed at different temperatures that show the charge separation is still sufficient to cause spatial separation of carriers and domain directed deposition.

The ferroelectric nature of PZT makes it attractive for a memory device. Therefore, by tracking the change in the photochemical reactivity we are also generating a handle for understanding the impact of trap and defect states on the electrical performance of the PZT, when for example in an FeRAM device.

4. Conclusion

We have shown that increasing the defect concentration in a sample of sol–gel derived PZT can enhance the deposition of photogenerated silver nanoparticles. When PZT samples were annealed in air at temperatures ranging from 530 to 690°C the silver nanoparticle deposition increased by more than 200% at the higher compared to the lower temperature. This increase in Ag deposition on the PZT surface is attributed to an increase in the defect concentration in the near surface region as a result of PbO evaporating from the surface. This leads to the development of more mobile carriers and decreases the width of space charge region. An additional change is the development of trap states associated with the oxygen vacancies that increases the time electrons spend at the interface and so enhances the photoconversion of metal cation into metal.

Acknowledgments

The authors wish to thank Dr. Qi Zhang for providing the PZT sols and Dr. Diego Gallardo for useful discussions.

References

[1]. Giocondi, J. L. and Rohrer, G. S., Spatially selective photochemical reduction of silver on the surface of ferroelectric barium titanate. ***Chemistry of Materials***, 2001, **13**, 241–242.

[2]. Kalinin, S. V., Bonnell, D. A., Alvarez, T., Lei, X., Hu, Z., Ferris, J. H. ***et al.***, Atomic polarization and local reactivity on ferroelectric surfaces: a new route toward complex nanostructures. ***Nano Letters***, 2002, **2**, 589–593.

[3]. Zhu, X. Y., Surface photochemistry. ***Annual Review of Physical Chemistry***, 1994, **45**, 113.

[4]. Kalinin, S. V. and Bonnell, D. A., ***Nanoscale phenomenon in ferroelectric thin films***. Kluwer Academic Publishers, Dordrecht, 2004.

[5]. Fridkin, V. M., ***Ferroelectric semiconductors***. Consultants Bureau, New York, 1980.

[6]. Jones, P. M. and Dunn, S., Photo-reduction of silver salts on highly heterogeneous lead zirconate titanate. ***Nanotechnology***, 2007, **18**, 185702–185707.

[7]. Dunn, S. and Tiwari, D., Influence of ferroelectricity on the photoelectric effect of $LiNbO_3$. ***Applied Physics Letters***, 2008, **93**, 092905–92911.

[8]. Hanson, J. N., Rodriguez, B. J., Nemanich, R. J. and Gruverman, A., Fabrication of metallic nanowires on a ferroelectric template via photochemical reaction. ***Nanotechnology***, 2006, **17**, 4946–4949.

[9]. Scott, J. F., ***Ferroelectric memories***. Springer, New York, 2000.

[10].Dunn, S., Tiwari, D., Jones, P. M. and Gallardo, D. E., Insights into the relationship between inherent materials properties of PZT and photochemistry for the development of nanostructured silver. ***Journal of Materials Chemistry***, 2007, **17**, 4460–4463.

[11].Yang, W., Rodriguez, B. J., Gruverman, A. and Nemanich, R. J., Polarization-dependent electron affinity of $LiNbO_3$ surfaces. ***Applied Physics Letters***, 2004, **85**, 2316–2318.

[12].Jones, P. M. and Dunn, S., Interaction of Stern layer and domain structure on photochemistry of lead–zirconate–titanate. ***Journal of Physics D: Applied Physics***, 2009, **42**, 065408.

[13].Zhang, Q. and Whatmore, R. W., Sol–gel PZT and mn-doped PZT thin films for pyroelectric applications. ***Journal of Physics D: Applied Physics***, 2001, **34**, 2296–2301.

[14].Dunn, S. and Whatmore, R. W., Transformation dependence of lead zir-conate titanate (PZT) as shown by PiezoAFM surface mapping of sol–gel produced PZT on various substrates. ***Integrated Ferroelectrics***, 2001, **38**, 39–47.

[15].Boerasu, I., Pintilie, L., Pereira, M., Vasilevskiy, M. I. and Gomes, M. J. M., Competition between ferroelectric and semiconductor properties in $Pb(Zr_{0.65}Ti_{0.35})O_3$ thin films deposited by sol–gel. ***Journal of Applied Physics***, 2003, **93**, 4776–4783.

[16].Kalinin, S. V., Bonnell, D. A., Alvarez, T., Lei, X., Hu, Z., Shao, R. ***et al.***, Ferroelectric lithography of multicomponent nanostructures. ***Advanced Materials***, 2004, **16**, 795–799.

[17].Smyth, D. M., Defect structure in perovskite titanates. ***Current Opinion in Solid State & Materials Science***, 1996, **1**, 692–697.

[18].Agrawwal, S. and Ramesh, R., Point defect chemistry of metal oxide het-erostructures. ***Annual Reviews Materials Science***, 1998, 28, 463–499.

[19].Robertson, J. and Warren, W. L., Energy levels of point defects in perovskite oxides. ***Proceedings of the 1994 MRS Fall Meeting***, 1995, 123–128.

[20].Ayguavives, F., Agius, A., Ea-Kim, B. and Vickridge, I., Oxygen transport during annealing of Pb(Zr,Ti)O3 thin films in O2 gas and its effect on their conductivity. ***Journal of Materials Research***, 2001, 16, 3005–3008.

[21].Xiao, Y., The influence of oxygen vacancies on domain patterns in ferroelec-tric perovskites. Ph.D. Thesis, California Institute of Technology, California, 2004.
[22].Lewis, N. S., Progress in understanding electron-transfer reactions at semi-conductor/liquid interfaces. ***Journal of Physical Chemistry B,*** 1998, 102, 4843–4855.



https://dspace.org/

Influence of annealing on the photochemical deposition of silver onto PZT thin films under UV irradiation

Tiwari, Divya; Dunn, Steve

2009-10-31T00:00:00Z
Elsevier Science B.V., Amsterdam.
http://dx.doi.org/10.1016/j.jeurceramsoc.2009.03.018
Divya Tiwari, Steve Dunn, Influence of annealing on the photochemical deposition of silver onto PZT thin films under UV irradiation, Journal of the European Ceramic Society, Vol. 29, Issue 13, October 2009, Pages 2799-2805, ISSN 0955-2219, http://dx.doi.org/10.1016/j.jeurceramsoc.2009.03.018.

Downloaded from a DSpace repository. https://dspace.org/